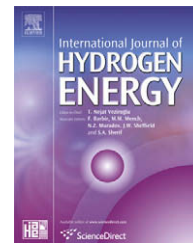


Available at www.sciencedirect.comjournal homepage: www.elsevier.com/locate/ijhe

Modeling and control design of hydrogen production process for an active hydrogen/wind hybrid power system

Tao Zhou*, Bruno Francois

L2EP, Ecole Centrale de Lille, Cite Scientifique, BP48, 59651, Villeneuve d'Ascq, France

ARTICLE INFO

Article history:

Received 4 August 2008

Received in revised form

1 October 2008

Accepted 2 October 2008

Available online 21 November 2008

Keywords:

Hybrid power system

Hydrogen production

Electrolyzer

Modeling

Control

Real-time simulation

ABSTRACT

This paper gives a control oriented modeling of an electrolyzer, as well as the ancillary system for the hydrogen production process. A Causal Ordering Graph of all necessary equations has been used to illustrate the global scheme for an easy understanding. The model is capable of characterizing the relations among the different physical quantities and can be used to determine the control system ensuring efficient and reliable operation of the electrolyzer. The proposed control method can manage the power flow and the hydrogen flow. The simulation results have highlighted the variation domains and the relations among the different physical quantities. The model has also been experimentally tested in real time with a Hardware-In-the-Loop Simulation before being integrated in the test bench of the active wind energy conversion system.

Crown Copyright © 2008 Published by Elsevier Ltd on behalf of International Association for Hydrogen Energy. All rights reserved

1. Introduction

Renewable energy sources (RES), as energy alternatives, have attracted special attention all over the world, in order to increase the security of energy supplies by reducing the dependency on imported fossil fuels and in order to reduce the emission of greenhouse gases. As a good candidate, the advancing wind power technologies have increased the use of wind energy conversion system (WECS) for distributed generation (from wind farms) to satisfy the grid energy demand [1–4]. However, the WECS depending entirely on the wind generators is a passive generator, which cannot offer any services to the grid since the wind is an intermittent energy source. As solutions, hybrid power systems (HPS) are proposed to overcome the problems with two innovative improvements:

- *Storage subsystems* are associated with the wind generator to compensate or absorb the difference between the generated wind power and the required grid power [5–7];
- *Energy management strategies* are needed to drive the power flows among the wind generator, the storage subsystems and the grid. It has to implement various additional control functions to provide auxiliary services for the grid [8–10].

As a result, the wind based HPS can offer some services to the grid (stable active and reactive power supply, voltage and frequency regulation, etc.) and become an active WECS.

In our studied HPS (Fig. 1), the wind generator and different storage units are connected to a common dc bus, which is connected to the grid through a power electronic inverter. Super-capacitors can be used for fast-dynamic storage

* Corresponding author. Tel.: +33 320 335385; fax: +33 320 335454.

E-mail addresses: tao.zhou@ec-lille.fr (T. Zhou), bruno.francois@ec-lille.fr (B. Francois).

Nomenclature			
u_{bus}	DC-bus voltage	m'_{el}	hydrogen evolution rate in the electrolyzer
i_{m_el}	modulated current of the buck converter	m'_{el_pro}	hydrogen production rate in the electrolyzer
u_{m_el}	modulated voltage of the buck converter	m'_{el_out}	hydrogen outlet rate from the electrolyzer
i_{Lel}	choke current	p_{el}	hydrogen pressure in the electrolyzer
d	duty ratio of the buck converter	T_{el}	temperature in the electrolyzer
i_{el}	electrolyzer stack current	R	universal gas constant ($R = 8.314$)
u_{el}	electrolyzer stack voltage	V_{el}	volume of the cathode
N_{el}	number of electrolyzer cells	P_{comp}	compressor power
u_{cell}	voltage across one electrolyzer cell	w	polytropic work
u_0	thermodynamic cell voltage	k	polytropic coefficient ($k = 1.4$)
r_i	parameters for ohmic resistance of electrolyte	p_{sto}	hydrogen pressure in the tank
s_i	parameters for overvoltage across electrodes	m'_{sto}	hydrogen evolution rate in the tank
t_i	parameters for overvoltage across electrodes	m'_{fc}	hydrogen outlet flow rate from the tank to fuel cell
A	area of the electrode	m'_{sto_leak}	hydrogen leakage rate from the tank
T_{el}	temperature of the electrolyte	T_{sto}	temperature in the hydrogen tank
F	Faraday constant ($F = 96485$)	V_{sto}	volume of the hydrogen tank
n	number of moles of transferred electrons ($n = 2$)	P_{bus_el}	electrical power transmitted to the electrolyzer
α_{el}	current efficiency of the electrolyzer	x_{ref}	reference value of x
a_i	parameters for current efficiency ($i = 1,2...5$)	\hat{x}	estimated value of x
		\bar{x}	measured value of x

because of their high power density and convenience for fast charging and discharging processing. The long-term storage in the form of hydrogen (H_2) is chosen because of its inherent high mass energy density. In the case of wind energy surplus, the electrolyzer converts the excess energy into H_2 by electro-chemical reaction. The produced H_2 can be stored in the hydrogen tank for the future re-utilization. In the case of wind energy deficit, the stored electrolytic H_2 can be re-used to generate the electricity by a proton exchange membrane fuel

cell to meet the energy demand of the grid. By using an electrolyzer, hydrogen conversion allows both storage and transportation of large amounts of power at much higher energy densities. Thus, hydrogen production contributes directly to the reduction of the dependence on imported fossil fuel [11,12]. According to Refs. [13,14], wind electrolysis is an attractive candidate for economically viable renewable-hydrogen production system. Furthermore, coupling wind turbines with electrolyzers has the potential to provide

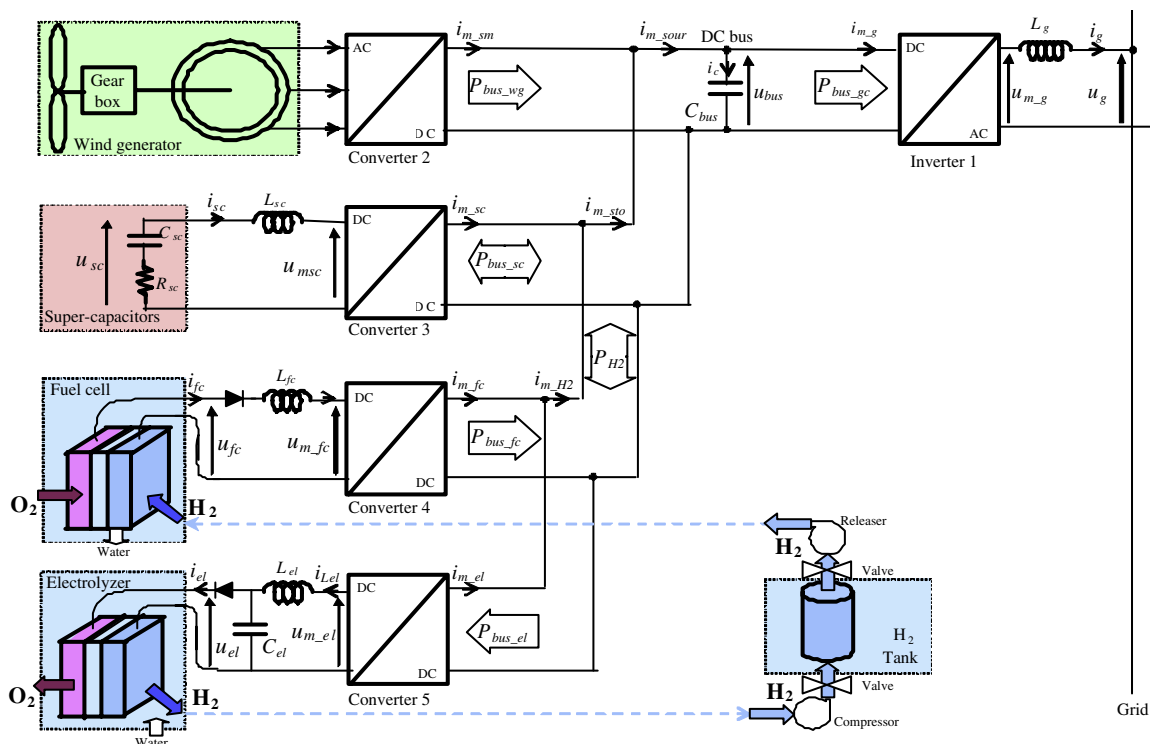


Fig. 1 – The studied hybrid power system based on wind energy and hydrogen technologies.

low-cost, environmentally friendly distributed generation of hydrogen in addition to electricity [11].

Some energy management strategies are implemented in the control system, for satisfying the grid requirements while maximizing the benefit of renewable energy sources and optimizing the operation of each storage unit. Specifically for electrolyzer, when the generated wind power is more than the required grid power, the electrolyzer should be properly controlled to follow a desired power reference profile in order to absorb the power difference with help of the super-capacitors.

In order to achieve the required performances of the electrolyzer system and its control, a test bench has been built based on the Hardware-In-the-Loop (HIL) emulations. Such HIL simulation can be used to test and compare the electrical behaviors of different electrolyzer technologies. It consists of two parts:

- the power electronic stage, which is used to supply the electrolyzer's power;
- the control stage, which is used for the power electronic device's control and the electrolyzer's behavior emulation by using mathematical modeling.

So the control stage is an important part, which determines the whole emulator's behavior.

The modeling of the electrolyzer has not yet been studied as widely as the fuel cell in the literature. In Ref. [15] the authors have developed a model for the unipolar stuart cell electrolyzer, by assuming a fixed temperature and a 100% current efficiency, which has also been used in Refs. [16,17]. The higher heating value (HHV) of the H_2 has also been used to give the theoretical model of the electrolysis process [18,19]. Much more electrolyzer current-voltage characteristics are obtained empirically by experimental measurements and show much dependence on pressure and temperature. Some of these empirical models use the "log" term [20,21] to describe the non-linear relations between the voltage and current, while others use the "ln" term [22–25]. Some models have also been modified for the ease of control and simulation purposes [26,27]. Electrolyzer models are generally formulated with the Faraday's Law, and the hydrogen production rate depends proportionally on the current. However, detailed relations and causality among the physical quantities in the hydrogen production system should be shown more clearly. The organization of the modeling equations should be suitable for an accurate dynamic simulation, for the control design and for the power management design together with the hydrogen production subsystem, including power conditioning system and hydrogen gas handling system.

In this paper, we focus on the hydrogen production system to explain how the electrolyzer absorbs the electrical energy and converts it into hydrogen. A detailed control oriented model is given by using a causal ordering graph for the electrolyzer, as well as for the other parts for the hydrogen production process. The model characterizes the relations among the different physical quantities and can be used to determine the control system ensuring efficient and reliable operation of the electrolyzer. This paper is organized as follows. The mathematical modeling of each part of the

hydrogen production process is presented in Section 2, with dc-dc converter, electrolyzer, compressor, and hydrogen tank. In Section 3, the control schemes are presented to manage the power flow and the hydrogen flow. The simulation results are presented in Section 4 and the relations among the different physical quantities are highlighted. An HIL emulator based on a real electrolyzer is presented in Section 5 to validate the modeling method and the conclusions are given in Section 6.

2. Modeling of the hydrogen production process

In this section, the Causal Ordering Graph (COG) is used to model the electrolyzer and its auxiliary equipment. To simplify the modeling, the gas is assumed to be dried and purified; all kinds of hydrogen leakage are assumed to be very small and can be neglected in the production, handling and storage processes. The power conditioning unit is performed by a power electronic converter (Converter 5 in Fig. 1), whose task is to adapt and tune electrical quantities of the electrolyzer with the DC bus (capacitor C_{bus}). The gas handling system can be modeled by a compressor, it supplies the necessary power to press the dry and purified hydrogen into the tank.

2.1. Presentation of the causal ordering graph

The COG is a graphical representation of mathematical equations, which is used to model a system and to design its control structure [28,29]. Balloons with an equation number represent modeling relations. A static instantaneous relation has no time dependence. It will be depicted as a balloon with a bi-directional arrow as shown in Fig. 2a. Physically, it can be said that the corresponding element has an external causality orientation. If the variable x is externally set, it is then the input and we get:

$$y(t) = R_a(x(t)). \quad (Ra)$$

To make the output y equal to a reference y_{ref} , an elementary control equation (R_{ac}) is obtained by inverting the modeling equation (R_a) to calculate the desired input variable x_{reg} from the reference y_{ref} .

$$x_{reg}(t) = R_{ac}(y_{ref}(t)). \quad (Rac)$$

A time-dependent relation will be characterized by a unidirectional arrow in the balloon. Classically, dynamical systems are mathematically modeled by differential equations,

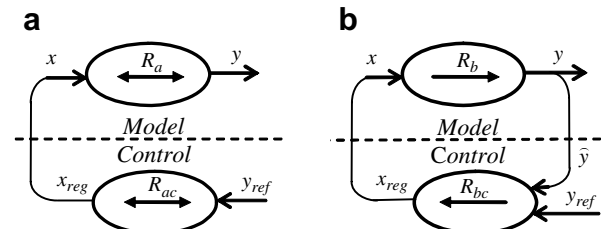


Fig. 2 – COG of static and dynamic relations with their control schemes. (a) static relation; (b) dynamic relation.

$dy(t)/dt = ax(t) + b$. This first order differential equation is typically a time-dependent relation, whose output is calculated by integration. It is represented by (R_b) in Fig. 2b,

$$y(t) = R_b(x(t), t), \tag{Rb}$$

Moreover the mathematical property of differential equations specifies that this equation type has an input–output orientation. Meanwhile for equation (R_b) , the variable $x(t)$ must be the input and $y(t)$ must be the output. Physically, it can be said that the element has an internal causality orientation. The pure inverse equation introduces large instabilities due to the differential term. Instead of inverting R_b , we can use a closed loop control with a corrector C_m to compensate the error signal between the measured output \hat{y} and the reference y_{ref} .

$$x_{reg}(t) = C_m(y_{ref}(t) - \hat{y}(t)). \tag{Rbc}$$

2.2. Modeling of the buck converter

Power electronic converters are usually used as power conditioning units. Since the voltage applied to the electrolyzer is lower than the DC-bus voltage, a so-called buck DC–DC converter is required to supply the electrolyzer by stepping down the DC-bus voltage. So the power transmitted to the electrolyzer can be regulated by controlling the buck converter at the control input, which is called duty ratio (the ratio of the power transistor’s ON-state time versus the switching period). The average model of the buck converter is accurate enough to describe the process and can be used to simplify the system modeling structure [30].

$$u_{m_el} = du_{bus} \tag{R1}$$

and

$$i_{m_el} = di_{Le1} \tag{R2}$$

where u_{bus} and i_{m_el} are respectively the DC-bus voltage and the modulated current of the buck converter; u_{m_el} is the modulated voltage and i_{Le1} is the choke current. The corresponding COG of the converter is shown in Fig. 3.

2.3. Modeling of the electrolyzer

The electrolyzer consumes the electrical power to produce hydrogen. Its modeling can be divided into four different parts: the electrical part, the electro-chemical part, the

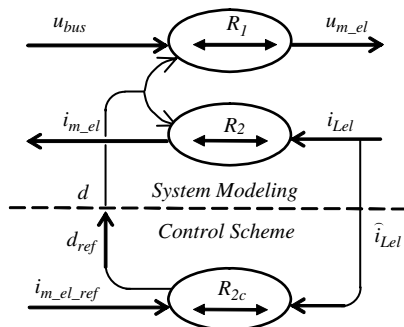


Fig. 3 – COG of the buck converter and the power flow control.

thermal part and the hydraulic part. The operation of the whole electrolyzer is based on the interaction among these four parts.

2.3.1. Electrical part

Most reported models of electrolyzers’ electrical behavior are obtained empirically by measurements [20–27]. Here, an adequate empirical model [20] is used to describe the characteristic of a given electrolyzer as shown in Fig. 4:

$$\begin{cases} u_{cell} = u_0 + \frac{r_1+r_2T_{el}}{A}i_{el} + (s_1 + s_2T_{el} + s_3T_{el}^2)\log\left(\frac{t_1+t_2/T_{el}+t_3/T_{el}^2}{A}i_{el} + 1\right) \\ u_{el} = N_{el}u_{cell} \end{cases} \tag{R3}$$

where N_{el} is the number of electrolyzer cells, u_{cell} is the voltage across one electrolyzer cell, i_{el} is the generated current of the electrolyzer, u_0 is the thermodynamic cell voltage varying slowly with the temperature and pressure, r_i are the parameters for ohmic resistance of electrolyte, s_i and t_i are the parameters for overvoltage on electrodes, A is the area of the electrode, and T_{el} is the temperature of the electrolyte. All parameters values have been identified by measurements (Table 1). This electrical characteristic depends mainly on the voltage, the current and the temperature. The non-linear current versus voltage relationship shows that the electrolyzer can be considered as a variable non-linear resistor. At a given temperature, the relationship between u_{el} and i_{el} is bijective (Fig. 4). The reciprocal relationship of the empirical model, which is described in R_3 can be found by linear interpolation with a wished accuracy, as shown in Fig. 5. It is named R_3^{-1} and can be implemented in a look-up table. Thus the current value i_{el} corresponding to each given voltage u_{el} can be easily obtained.

$$i_{el} = F(u_{el}) \tag{R3 - 1}$$

2.3.2. Electro-chemical part

The electro-chemical reactions in water electrolysis can be summarized in Table 2. According to the Faraday’s law, the hydrogen production rate m'_{el_pro} depends on the electrolyzer current,

$$m'_{el_pro} = \alpha_{el}(T_{el}, i_{el}) \frac{N_{el}}{nF} i_{el} \tag{R4}$$

where F is the Faraday constant and n is the number of moles of transferred electrons per mole of water. The current

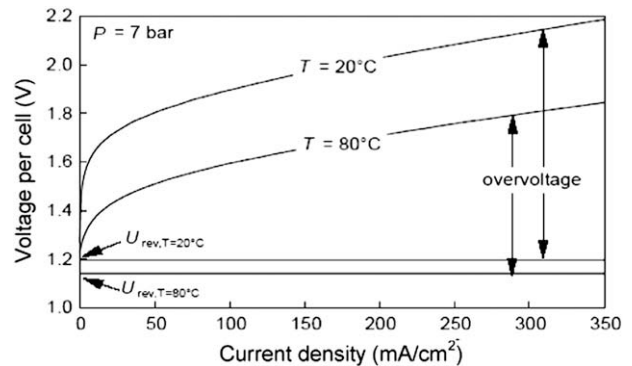


Fig. 4 – Typical I–U characteristics of an electrolyzer cell (R_3) [20].

Table 1 – Parameters of the electrolyzer model [20].

r_1	7.3e-5	$\Omega \text{ m}^2$	r_2	-1.1e-7	$\Omega \text{ m}^2/\text{C}$
s_1	1.6e-1	V	s_2	1.38e-3	V/C
s_3	-1.6e-5	V/C^2	t_1	1.60e-2	m^2/A
t_2	-1.3	$\text{m}^2 \cdot \text{C}/\text{A}$	t_3	4.12e2	$\text{m}^2 \cdot \text{C}^2/\text{A}$
A	0.25	m^2	a_1	99.5%	
a_2	-9.58	m^2/A	a_3	-0.056	$\text{m}^2/\text{A}/\text{C}$
a_4	1502.7	m^4/A	a_5	-70.8	$\text{m}^4/\text{A}/\text{C}$
N_{el}	21		T_{el}	25	$^{\circ}\text{C}$

efficiency α_{el} varies also with the electrolyzer current density. The relation can be described by an empirical expression:

$$\alpha_{\text{el}} = a_1 \exp\left(\frac{a_2 + a_3 T}{i_{\text{el}}/A} + \frac{a_4 + a_5 T}{(i_{\text{el}}/A)^2}\right)$$

where the parameters a_i ($i=1,2,\dots,5$) are calculated from measurements and are given in Table 1.

2.3.3. Thermal part

The electrolyte temperature affects both the I-U curve and the Faraday efficiency. It can be determined by using simple (calculated from a quasi-static thermal model) or complex (calculated from a lumped thermal capacitance model) thermal models depending on the required accuracy. Since the time constant in the thermal domain is much larger than in the other physic domains, we assume a constant temperature T_{el} , which can be set externally, to substitute the thermal model.

2.3.4. Hydraulic part

If we ignore the hydrogen leakage rate from the electrolyzer, the hydrogen evolution rate m'_{el} in the cathode depends on both the production rate $m'_{\text{el,pro}}$ and the outlet rate $m'_{\text{el,out}}$:

$$m'_{\text{el}}(\tau) = m'_{\text{el,pro}}(\tau) - m'_{\text{el,out}}(\tau). \quad (\text{R5})$$

The stored hydrogen quantity can be described as follows:

$$m_{\text{el}}(t_0 + \Delta t) = \int_{t_0}^{t_0 + \Delta t} m'_{\text{el}}(\tau) d\tau + m_{\text{el}}(t_0) \quad (\text{R6})$$

The hydrogen pressure in the electrolyzer can be found with the ideal gas law,

$$p_{\text{el}} = \frac{RT_{\text{el}}}{V_{\text{el}}} m_{\text{el}}, \quad (\text{R7})$$

where p_{el} and T_{el} are respectively the hydrogen pressure and temperature in the electrolyzer, R is the universal gas constant

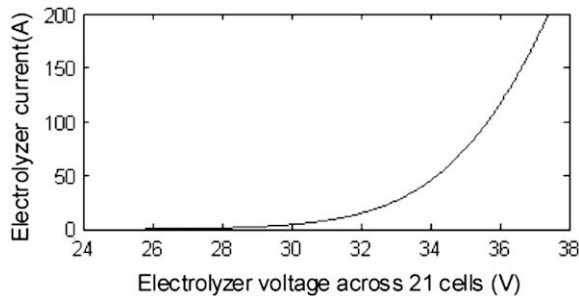


Fig. 5 – The reciprocal relationship (R_3^{-1}) curve from u_{el} to i_{el} obtained by linear interpolation for a given $T_{\text{el}} = 25^{\circ}\text{C}$.

and V_{el} is the volume of the cathode. In steady-state operation, the hydrogen outlet rate should be regulated to be equal to the hydrogen production rate and the stored hydrogen quantity in the cathode should be maintained constant as well as the pressure. The COG of the electrolyzer shows the organization of all modeling equations (Fig. 6).

2.4. Modeling of the compressor

The compressor is based on a polytropic compression process. The relationship between the hydrogen molar flow rate (considered equal to the outlet rate from the electrolyzer $m'_{\text{el,out}}$) and the compressor power P_{comp} is:

$$m'_{\text{el,out}} = \frac{\alpha_{\text{comp}} P_{\text{comp}}}{w}, \quad (\text{R8})$$

and

$$w = \frac{kRT_{\text{el}}}{k-1} \left[\left(\frac{p_{\text{sto}}}{p_{\text{el}}} \right)^{\frac{k-1}{k}} - 1 \right], \quad (\text{R9})$$

where w is the polytropic work, α_{comp} is the compressor efficiency, k is the polytropic coefficient, T_{el} is the inlet gas temperature, p_{el} is the inlet gas pressure, corresponding to the hydrogen pressure in the electrolyzer, p_{sto} is the outlet gas pressure, corresponding to the hydrogen pressure in the tank. The corresponding COG can be derived (Fig. 7).

2.5. Modeling of the hydrogen tank

The stored hydrogen rate m'_{sto} depends on three terms: the input flow rate $m'_{\text{el,out}}$ outlet from the electrolyzer, the outlet flow rate m'_{fc} to the fuel cell and the leakage rate $m'_{\text{sto,leak}}$ to the environment,

$$m'_{\text{sto}}(\tau) = m'_{\text{el,out}}(\tau) - m'_{\text{fc}}(\tau) - m'_{\text{sto,leak}}(\tau).$$

Since the electrolyzer and the fuel cell never work at the same time for efficiency reasons, the outlet flow rate from the electrolyzer is zero. If we neglect the leakage, the number of moles, which are stored in the tank m_{sto} can be expressed as:

$$m_{\text{sto}}(t_0 + \Delta t) = \int_{t_0}^{t_0 + \Delta t} m'_{\text{el,out}}(\tau) d\tau + m_{\text{sto}}(t_0) \quad (\text{R10})$$

The pressure in the hydrogen tank can be derived from the Van der Waals equation of state for real gases. But for the ease of the modeling, we use the ideal gas law:

$$p_{\text{sto}} = \frac{RT_{\text{sto}}}{V_{\text{sto}}} m_{\text{sto}}, \quad (\text{R11})$$

where T_{sto} is the gas temperature, V_{sto} is the storage tank volume. The COG of the hydrogen tank is shown in Fig. 8.

2.6. Modeling of the hydrogen production process

We consider that the DC bus is equivalent to an ideal voltage source supplying a constant voltage u_{bus} . Thus, the variation of the electrical power consumed by the electrolyzer $P_{\text{bus,el}}$ due to the intermittent wind energy can be expressed by the variation of the current $i_{\text{m,el}}$. Each ‘‘System Modeling’’ part of the presented COGs can be considered as a block with several inputs and outputs. If they are connected together by the corresponding inputs and outputs, a macroscopic

Table 2 – Electro-chemical reactions in water electrolyzers.

Electrolyte reaction	Anode reaction	Cathode
Alkaline (KOH)	$2\text{OH}^- (\text{aq}) \rightarrow \frac{1}{2}\text{O}_2 (\text{g}) + \text{H}_2\text{O} + 2\text{e}^-$	$2\text{H}_2\text{O} (\text{l}) + 2\text{e}^- \rightarrow \text{H}_2 (\text{g}) + 2\text{OH}^- (\text{aq})$
Acidic (SPE)	$\text{H}_2\text{O} (\text{l}) \rightarrow \frac{1}{2}\text{O}_2 (\text{g}) + 2\text{H}^+ (\text{aq}) + 2\text{e}^-$	$2\text{H}^+ (\text{aq}) + 2\text{e}^- \rightarrow \text{H}_2 (\text{g})$

representation of the hydrogen production process can be obtained, as shown in Fig. 9a. The blocks with a dotted line represent the parts where some time-dependent relation can be found and correspond to some process with energy accumulations. The temperatures, such as T_{el} and T_{sto} are assumed to be controlled by a thermostatic system. From the macro representation, it is obviously shown that the duty ratio d and the compressor power P_{comp} are the control inputs, which can be used to regulate the consumed power ($P_{bus,el} = u_{bus} \cdot i_{m,el} = u_{el} \cdot i_{el} = P_{el}$) and the gas flow during the hydrogen production process.

3. Control of the hydrogen production process

3.1. General principles

The design of the control system is based on the inversion of the ‘‘System Modeling’’ parts of all COGs. The purposes of the control system are to absorb the excess electrical power (which is produced by the wind generator) into hydrogen and to send the produced hydrogen gas towards the tank, by keeping the H_2 pressure (p_{el}) constant in the electrolyzer for security and efficiency reasons. The whole control scheme consists of the following functions (Fig. 9a):

- a current controller, which guarantees the desired power flow by controlling the modulated current $i_{m,el}$ through the desired duty ratio d_{ref} of the buck converter;
- an electrolyzer pressure controller, which maintains a constant H_2 pressure p_{el} in the electrolyzer by determining a desired H_2 outlet rate $m'_{el,out,ref}$ (it must be equal to the H_2 production rate $m'_{el,pro}$ depending on the electrolyzer current i_{el});

- a hydrogen flow controller, which drives the H_2 at the desired flow rate $m'_{el,out,ref}$ by supplying the necessary compression power $P_{comp,ref}$.

3.2. Buck converter controller

Various objectives for the control of the buck converter can be considered and will result in various control functions. As for example, the objective can be to control the electrolyzer voltage to a prescribed value. Here for the ease of explanation, the objective is to control the electrolyzer power. Since the DC bus is considered as an ideal DC source with a constant voltage u_{bus} , the variation of the electrical power $P_{bus,el}$ transmitted to the electrolyzer can be expressed by the variation of the current $i_{m,el}$,

$$\Delta P_{bus,el}(t) = u_{bus} \Delta i_{m,el}(t).$$

Therefore, the power regulation can be performed by a current controller. Since the relation (R_2) between the modulated current $i_{m,el}$ of the converter and the inductor current $i_{l,el}$, the current control algorithm can be given by inverting (R_2):

$$d_{ref} = \frac{i_{m,el,ref}}{\hat{i}_{l,el}} \tag{R2c}$$

where $\hat{i}_{l,el}$ is the sensed value of the current. The COG of the control of the current is shown in Fig. 3.

3.3. Pressure controller

For a desired working condition, the H_2 pressure p_{el} should be set at a wished level. Thus, the hydrogen outlet flow rate $m'_{el,out}$ from the electrolyzer should be equal to the hydrogen production rate $m'_{el,pro}$ in the electrolyzer, in order to set a constant number of moles m_{el} , as well as the pressure p_{el} according to equation (R_7). However, the molar flow rate

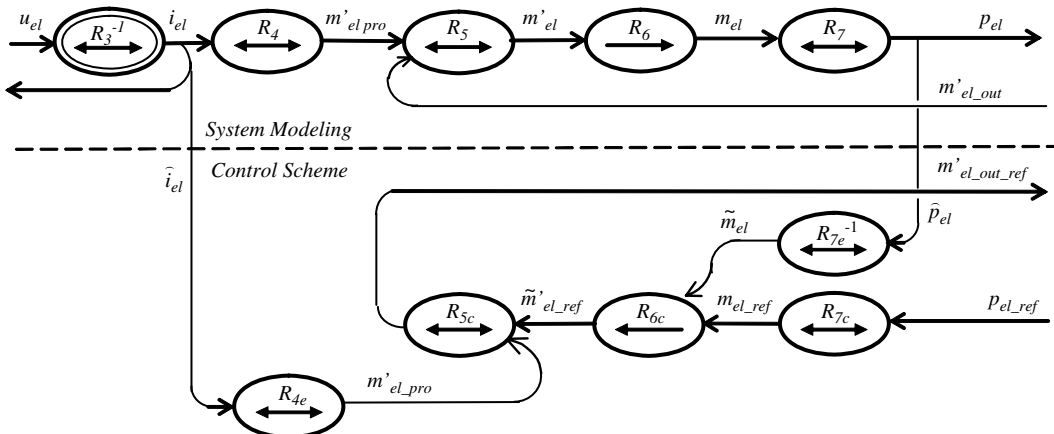


Fig. 6 – COG of the electrolyzer model and its pressure control.

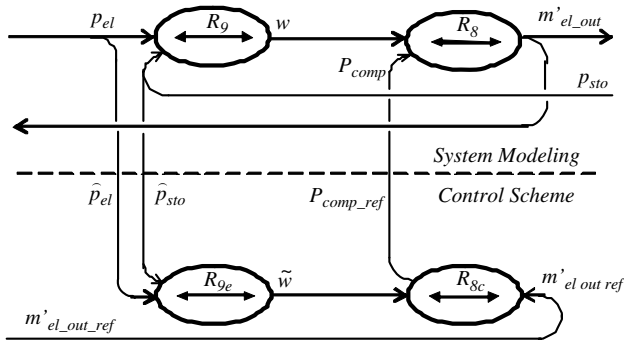


Fig. 7 – COG of the compressor model and the hydrogen flow control.

cannot be easily measured. Since the constant pressure is the equivalent consequence of the H₂ flow rate control, we can try to make the reference outlet rate $m'_{el_out_ref}$ to converge to the production rate m'_{el_ref} in order to maintain the wished constant pressure p_{el_ref} .

By inverting equation (R₇) (Fig. 6), the desired hydrogen number of moles m_{el_ref} and the estimation of the number of moles \tilde{m}_{el} can be deduced directly from the reference pressure p_{el_ref} and the measured pressure \hat{p}_{el} :

$$m_{el_ref} = \frac{V_{el}}{RT_{el}} p_{el_ref} \quad R7c$$

$$\tilde{m}_{el} = \frac{V_{el}}{RT_{el}} \hat{p}_{el} \quad R7e$$

Then, the reference hydrogen variation rate m'_{el_ref} in the electrolyzer can be obtained through a closed loop control with a corrector C_m ,

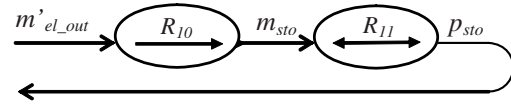


Fig. 8 – COG of the hydrogen storage model.

$$m'_{el_ref} = C_m (m_{el_ref} - \tilde{m}_{el}) \quad (R6c)$$

The reference of the hydrogen outlet flow rate $m'_{el_out_ref}$ from the electrolyzer can be obtained by inverting (R₅),

$$m'_{el_out_ref} = m'_{el_pro} - m'_{el_ref} \quad (R5c)$$

The estimated hydrogen production rate \tilde{m}'_{el_pro} is deduced directly from the sensed electrolyzer current \hat{i}_{el} (R₄):

$$\tilde{m}'_{el_pro} = \tilde{\alpha}_{el}(T_{el}, \hat{i}_{el}) \frac{N_{el}}{nF} \hat{i}_{el}, \quad (R4e)$$

where the estimated current efficiency $\tilde{\alpha}_{el}$ can also be obtained from the sensed electrolyzer current \hat{i}_{el} :

$$\tilde{\alpha}_{el} = a_1 \exp \left(\frac{a_2 + a_3 T}{\hat{i}_{el}/A} + \frac{a_5 + a_6 T}{(\hat{i}_{el}/A)^2} \right).$$

3.4. Hydrogen flow controller

The role of the compressor is to drive the hydrogen to the tank at the reference outlet flow rate $m'_{el_out_ref}$. The desired compressor power P_{comp_ref} can be calculated by inverting (R₈):

$$P_{comp_ref} = \frac{\tilde{w}}{\alpha_{comp}} m'_{el_out_ref}, \quad (R8c)$$

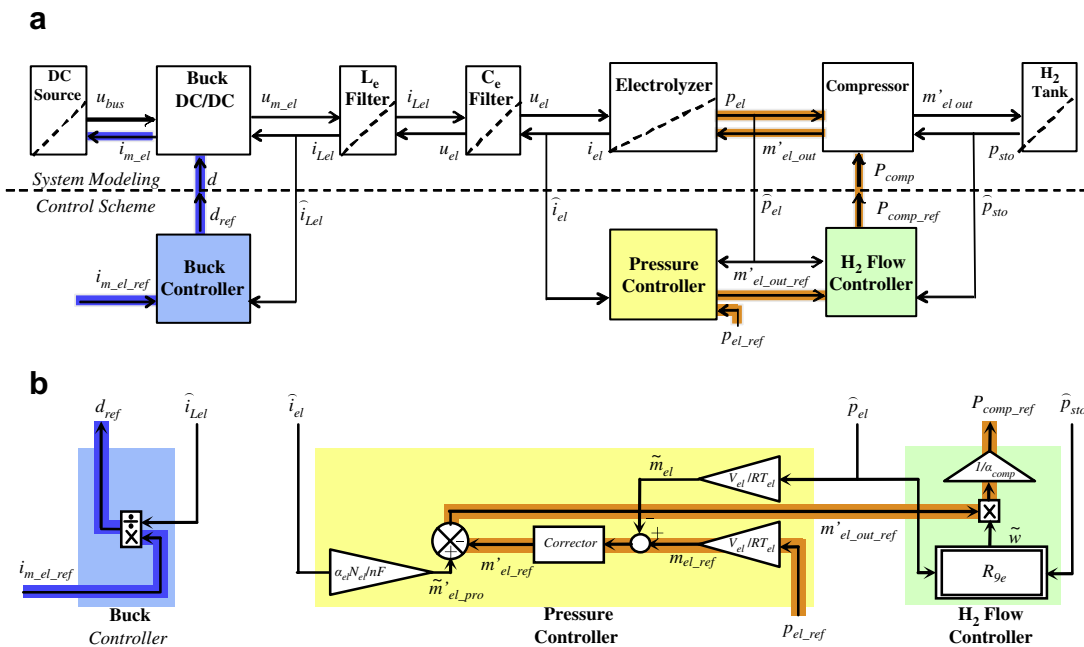


Fig. 9 – Representation of the system modeling and the control scheme of the hydrogen production process. (a) Macroscopic representation of the system modeling with the control scheme of the hydrogen production process; (b) Representation of the system modeling and the control scheme of the hydrogen production process.

where the value of the polytropic work \tilde{w} is estimated with the measured pressures \hat{p}_{sto} and \hat{p}_{el} ,

$$\tilde{w} = \frac{kRT_{el}}{k-1} \left[\left(\frac{\hat{p}_{sto}}{\hat{p}_{el}} \right)^{\frac{k-1}{k}} - 1 \right] \quad (R9e)$$

The COG of the hydrogen flow control is shown in Fig. 7.

3.5. The entire control scheme

When we gather all COGs, the macroscopic representation of the whole system model with its entire control scheme can be obtained, as shown in Fig. 9a. An equivalent block diagram for control representation is shown in Fig. 9b.

4. Simulation of the hydrogen production process

The model of this system is simulated with the presented control scheme in Matlab/Simulink™, with $u_{bus} = 48$ V, $T_{el} = 25$ °C, $V_{el} = 1$ L, $V_{sto} = 5$ L and the initial pressures $p_{el} = 3$ bar and $p_{sto} = 20$ bar. The compressor efficiency is assumed equal to 63%. It is widely accepted that one of the main weak points of the electrolyzer is its time constant, which depends on the auxiliary systems. As well known, by omitting all kinds of losses, the supplied power corresponds directly to the hydrogen production rate. If the power variation is faster than the gas delivery control capacity, the hydrogen pressure in the electrolyzer can no longer be controlled and some security problems will occur. Therefore, in practice, power slopes are always given for transients. Since the slope is limited much slower than the gas handling dynamic, the static models of the electrolyzer and compressor are enough to show the behavior of the hydrogen production process in this quasi-static working condition. In Ref. [31], a 20 kW alkaline electrolyzer can increase its power from 16% to 100% of its normal power within 40 s, nearly 500 W/s. And in our study, we give a power slope of 125 W/s, converted in current reference $i_{m,el,ref}$ (Fig. 10a).

The time evolutions of the physical quantities and the relation among these quantities have been clearly shown in Fig. 10. The duty ratio d depends directly on the current reference $i_{m,el,ref}$ through the control law (Fig. 10b). The electrolyzer voltage u_{el} depends on such a varying duty ratio (Fig. 10c), since the dc-bus voltage u_{bus} is nearly constant. The electrolyzer current i_{el} depends on the electrolyzer voltage u_{el} according to electrolyzer model equations (Fig. 10d). Since the hydrogen production rate is proportional to the electrolyzer current through the Faraday law, the hydrogen outlet rate $m'_{el,out}$ (Fig. 10e) is regulated and is equal to the hydrogen production rate (in steady state) by the compressor power P_{comp} (Fig. 10h) in order to maintain the pressure p_{el} constant (Fig. 10f). As a result, the hydrogen pressure p_{sto} (Fig. 10g) in the tank depends on the hydrogen outlet rate from the electrolyzer $m'_{el,out}$.

5. Experimental results with the electrolyzer emulator

A Hardware-In-the-Loop emulator of the electrolyzer has been designed with experimental data from a PHOEBUS advanced

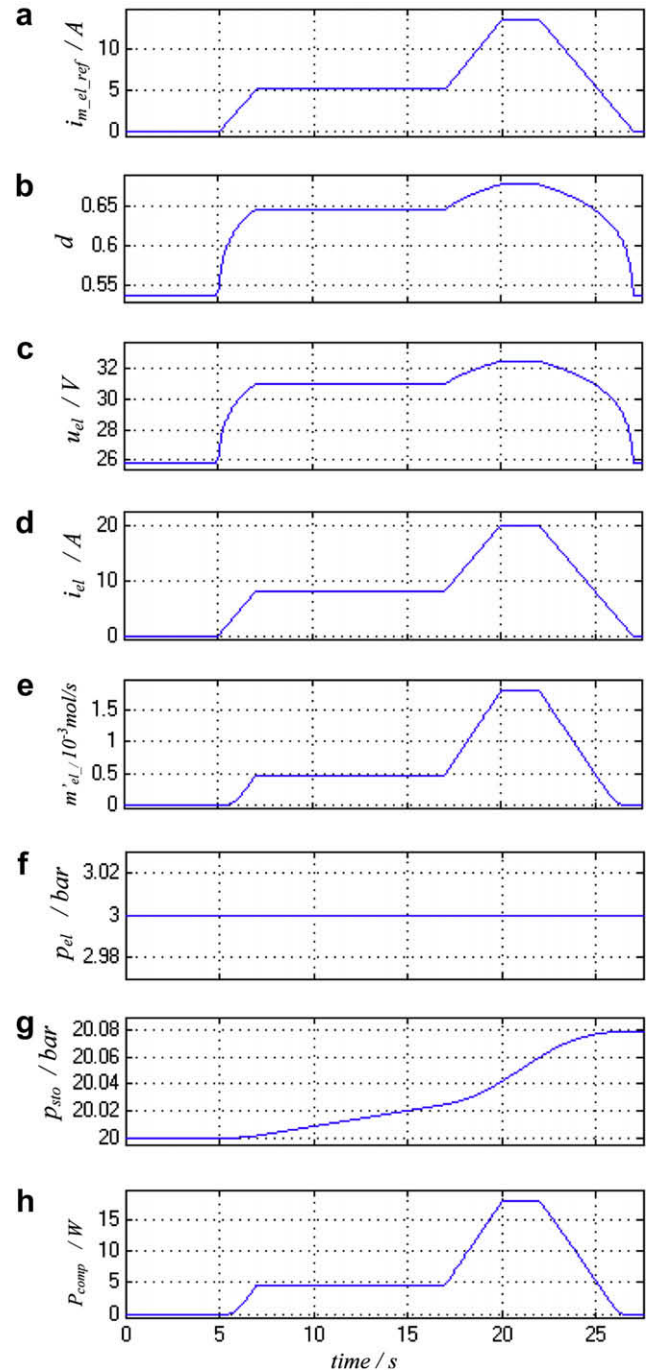


Fig. 10 – Simulation results of the response to the power slope.

alkaline electrolyzer [32]. The cells are circular, bipolar, they have a zero spacing geometry and they consist of NiO diaphragms and activated electrodes, which make them highly efficient. It can offer in real time the same terminal electrical characteristics as a real electrolyzer and so is used to test the active wind energy conversion system (Fig. 11a). Such an electrolyzer emulator can enable the test and comparison of the different electrolyzer devices with their corresponding mathematical models given by the manufacturer. Moreover, for studying the power management strategies of the hybrid

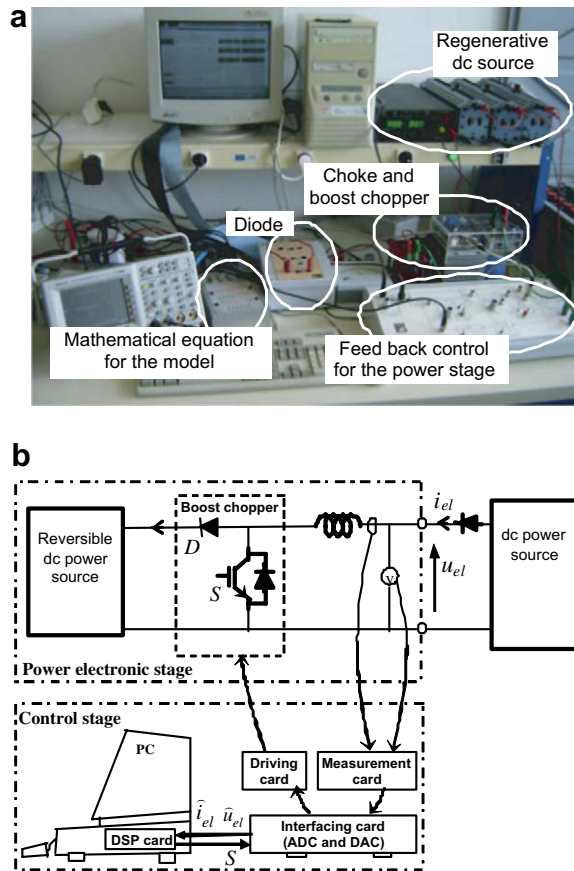


Fig. 11 – Electrolyzer emulator's schematic diagram.
(a) Hardware-In-the-Loop emulator of the electrolyzer;
(b) Structure of the electrolyzer emulator.

power system, it can be enough to use such an emulator instead of a real expensive electrolyzer.

The used electrolyzer emulator can be divided into two stages: the power electronic stage and the control stage (Fig. 11b). The power electronic stage consists of a boost dc/dc converter with an ideal regenerative source. It is designed to set the same current i_{el} as for a real electrolyzer. The control stage consists of the chopper's driving card, the measurement instruments, the Digital Signal Processing (DSP) card and the interfacing card. The software of the emulator is implemented in the DSP card. A feed-back closed loop is used to control the equivalent electrolyzer current i_{el} . The current reference i_{el_ref} is calculated from the electrolyzer model and pressure

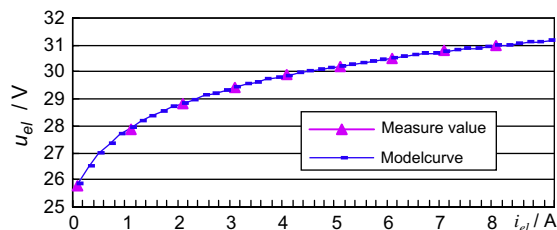


Fig. 12 – Comparison of the emulator's sensed data with the electrolyzer's static characteristic.

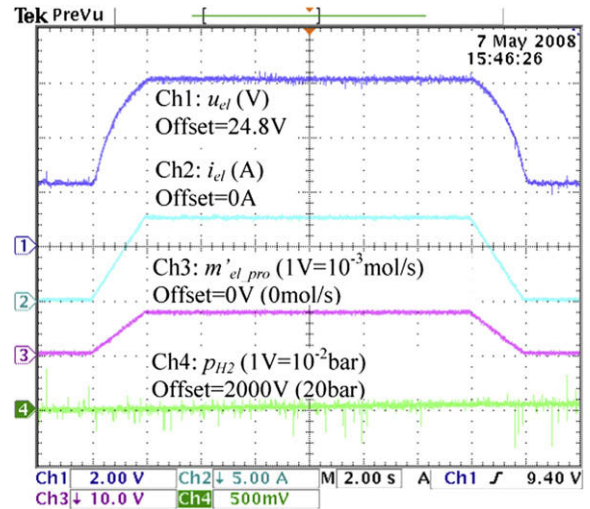


Fig. 13 – Electrolyzer emulator's response to power slope.

controller parts (Fig. 9), with a given pressure reference and the sensed voltage value \hat{u}_{el} . The static electrical characteristic R_3^{-1} with 21 cells of 0.25 m^2 has been implemented with the same parameters as used in the simulation above. We can see that the obtained emulator's static characteristic corresponds well to the model curve (Fig. 12).

When we give the same power slope variation to the emulator as in the simulation (from $t=0 \text{ s}$ to $t=17 \text{ s}$), the emulator can run in the quasi-static condition with the given temperature and pressure. The electrolyzer emulator's terminal response corresponds to the simulation results presented previously (Fig. 13).

Different auxiliary system models and their control algorithms can also be implemented in the DSP card, according to different purposes and methods. For example, we can implement the auxiliary system's model described above, to establish the relation between the electrolyzer and the hydrogen storage. The variation of the different physical quantities can also be simulated in the DSP card and verified via the computer desk in real time, such as the hydrogen outlet flow rate m'_{H2_out} by using the computed equation R_3^{-1} , and the hydrogen pressure p_{sto} in the storage by using the computed equations (R_{10}) and (R_{11}), etc.

6. Conclusions

First, a control oriented modeling of an electrolyzer, as well as the auxiliary system for the hydrogen production process has been presented by using a Causal Ordering Graph. The model is able to characterize the relations among the different physical quantities and can be used to determine the control system ensuring an efficient and reliable operation of the electrolyzer. The proposed control method can regulate the power flow and the hydrogen flow. With a slow power slope, the system can be considered in a quasi-static state, and the temperature can be considered constant, with external thermostatic system. We need to measure only a few quantities to correct the two control inputs: the duty ratio d and the compressor power

P_{comp} . The simulation results have highlighted the variation domains and dynamics of physical quantities.

Secondly, a HIL emulation of this hydrogen production process has been presented. This real-time emulator is based on a PHOEBUS advanced alkaline electrolyzer. It consists of a power electronic stage and a control stage. The power electronic stage can offer the same electrical characteristics as the real electrolyzer, with the help of the power converter control algorithms and the modeling equations of the electrolyzer system implemented in the control board. Such an electrolyzer emulator can help to test assessment of an active wind energy conversion system in the future.

Acknowledgment

This work has been supported by the French National Agency of the Research (ANR SuperEner Project) and the China Scholarship Council (CSC).

REFERENCES

- [1] Segura I, Pérez-Navarro A, Sánchez C, Ibáñez F, Payá J, Bernal E. Technical requirements for economical viability of electricity generation in stabilized wind parks. *Hydrogen Energy* Nov 2007;32(16):3811–9.
- [2] Fernandez RD, Battaiotto PE, Mantz RJ. Impact of wind farms voltage regulation on the stability of the network frequency. *Hydrogen Energy* July 2008;33(13):3543–8.
- [3] Obara S. Analysis of a fuel cell micro-grid with a small-scale wind turbine generator. *Hydrogen Energy* March 2007;32(3):323–36.
- [4] El Aïmani S, Minne F, François B, Robyns B. Modeling and simulation of doubly fed induction generators for variable speed wind turbines integrated in a distribution network”, In: 10th European conference on power electronics and applications, EPE’03, Sep. 2003, Toulouse (France), CD. ISBN 90-75815-07-7.
- [5] Abbey C, Joos G. Supercapacitor energy storage for wind energy applications. *IEEE Transactions on Industrial Electronics* May 2007;43(3):769–76.
- [6] Taljan G, Fowler M, Cañizares C, Verbič G. Hydrogen storage for mixed wind–nuclear power plants in the context of a hydrogen economy. *Hydrogen Energy* Sep 2008;33(17):4463–75.
- [7] Little M, Thomson M, Infield D. Electrical integration of renewable energy into stand-alone power supplies incorporating hydrogen storage. *Hydrogen Energy* July–August 2007;32(10–11):1582–8.
- [8] Tekin M, Hissel D, Pera MC, Kauffmann JM. Energy-management strategy for embedded fuel-cell systems using fuzzy logic. *IEEE Trans Ind Electron* Feb 2007;54(1):595–603.
- [9] Thounthong P, Rael S, Davat B. Control strategy of fuel cell and supercapacitors association for a distributed generation system. *IEEE Transactions on Industrial Electronics* Dec 2007;54(6):3225–33.
- [10] Zhou T, Lu D, Fakhm H, Francois B. Power flow control in different time scales for a wind/hydrogen/super-capacitors based active hybrid power system. In: EPE-PEMC’08, Poznan, Poland, Sep 2008, CD-ROM.
- [11] U.S. Department of Energy. Energy efficiency and renewable energy,” wind & hydropower technologies program, wind energy research area. Available from: <<http://www.eere.energy.gov>>.
- [12] Lebbal M, Zhou T, Francois B, Lecoeuche S. Dynamically electrical modelling of electrolyzer and hydrogen production regulation. In: International hydrogen energy congress and exhibition, IHEC 2007, Istanbul, Turkey; Jul.2007.
- [13] Dell RM, Rand DAJ. Energy storage—a key technology for global energy sustainability. *Power Sources* Nov 2001;100(1–2):2–17.
- [14] Shakyaa BD, Ayea Lu, Musgrave P. Technical feasibility and financial analysis of hybrid wind-photovoltaic system with hydrogen storage for Cooma. *Hydrogen Energy* Jan 2005;30(1):9–20.
- [15] Sapru K. Development of a small scale hydrogen production-storage system of hydrogen applications. In: IECEC ; 27 July–1 Aug 1997:3. p.1947–52.
- [16] Iqbal MT. Simulation of a small wind fuel cell hybrid energy system. *Renewable Energy* April 2003;28(4):511–22.
- [17] El-Shatter Th F, Eskandar MN, El-Hagry MT. Hybrid PV/fuel cell system design and simulation. *Renewable Energy* November 2002;27(3):479–85.
- [18] Hamelin J, Agbossou K, Laperrière A, Laurencelle F, Bose TK. Dynamic behavior of a PEM fuel cell stack for stationary applications. *Hydrogen Energy* June 2001;26(6):625–9.
- [19] Korpas M, Holen AT. Operation planning of hydrogen storage connected to wind power operating in a power market. *Transactions on Energy Conversion* Sep 2006;21(3):742–9.
- [20] Ulleberg Ø. Modeling of advanced alkaline electrolyzers: a system simulation approach. *Hydrogen Energy* Jan 2003;28(1):21–33.
- [21] Boccaletti C, Di Grazia G, Fabbri G, Nisticò E. Energy models for stand alone power systems. In: EETI 2004, Rio de Janeiro, Brazil; Oct 2004.
- [22] Vanhanen JP, Lund PD. Computational approaches for improving seasonal storage systems based on hydrogen technologies. *Hydrogen Energy* July 1995;20(7):575–85.
- [23] Agbossou K, Kolhe M, Hamelin J, Bose TK. Performance of a stand-alone renewable energy system based on energy storage as hydrogen. *IEEE Transactions on Energy Conversion* Sep 2004;19(3):633–40.
- [24] Kélouwani, Agbosso K, Chahine R. Model for energy conversion in renewable energy system with hydrogen storage. *Power Sources* Feb 2005;140(2):392–9.
- [25] Santarelli M, Pellegrino D. Mathematical optimization of a RES-H2 plant using a black box algorithm. *Renewable Energy* Apr 2005;30(4):493–510.
- [26] Bilodeau A, Agbossou K. Control analysis of renewable energy system with hydrogen storage for residential applications. *Power Sources* 22 Nov 2006;162(2):757–64.
- [27] Görgün H. Dynamic modelling of a proton exchange membrane (PEM) electrolyzer. *Hydrogen Energy* Jan 2006;31(1):29–38.
- [28] Guillaud X, Degobert P, Hautier J.P. Modeling control and causality : the causal ordering graph. In: 16th IMACS Control Engineering, Lausanne CD ROM; 2000.
- [29] Guillaud X, Francois B. A causal method for the modelling of static converter and the control design: application to a voltage source converter. In: EPE 2003, CD, Toulouse, France; September 2003.
- [30] Robyns B, Pankow Y, Leclercq L, François B. Equivalent continuous dynamic model of renewable energy systems. In: 7th international conference on modeling and simulation of electric machines, converters and systems; Electrimacs 2002.
- [31] Menzl F, Wenske M. Investigation of the steady state and transient operating behaviour of a 20 kW pressure electrolyser. In: Hypothesis II, Grimstad, Norway; 1997.
- [32] Ulleberg Ø. “Stand-alone power systems for the future: optimal design, operation & control of solar-hydrogen energy systems, PhD thesis. Norwegian University of Science and Technology; 1998.